# Effect of Gamma Irradiation Induced Modifications in Tungsten Oxide Thin Films and Their Potential Applications

Deepika[a], Deepika Gupta[a], Vishnu Chauhan[a], S K Sharma[b], Satyendra Kumar[c], & Rajesh Kumar[a*]

[a]University School of Basic and Applied Sciences, Guru Gobind Singh Indraprastha University, New Delhi 110 078, India
[b]University School of Information and Communication Technology, Gautam Buddha University, Greater Noida 201 312, India
[c]Department of Applied Science & Humanities, ABES Engineering College, Ghaziabad 201 009, India

In this work, we study the effect of high gamma doses (600 kGy, 1000 kGy and 1250 kGy) on morphological, structural and optical characteristics of sputtered $WO_3$ thin films. The modifications in these characteristics were analyzed by X-Ray Diffraction, Atomic Force Microscope, UV–Visible spectroscopy, Photoluminescence spectroscopy and Raman spectroscopy. AFM shows the variation in grain size from 61 nm to 91.2 nm after gamma irradiation from unirradiated to gamma-exposed $WO_3$ thin films. XRD and Raman spectroscopy show the monoclinic structure before and after irradiation of $WO_3$ thin films. The optical study illustrates the variation in the optical band gap from 2.80 eV to 2.08 eV after gamma exposure of $WO_3$ thin films. In PL spectra, two emission peaks at a wavelength of 410 nm and 480 nm were observed.

**Keywords:** Thin films, RF Sputtering, Gamma Irradiation, Atomic force microscope (AFM), X-Ray Diffraction (XRD), Raman Spectroscopy

## 1 Introduction

In the last decades, aqueous chemical dosimetry has been replaced by new radiation dosimeters and several studies show the influence of gamma doses on traits of metal oxide semiconductors[1]. In material science and device fabrication, radiation detection is a big problem observed. Recently, several metal oxides have been used for radiation detection. Among all the metal oxides, tungsten oxide ($WO_3$) is an n-type semiconductor having a band gap value from 2.7 eV to 3.3 eV is observed to be significant for a variety of applications such as gas sensors, electrochromic devices, biosensors, supercapacitors because of its peculiar physical properties, chemical stability and its non-toxicity[2]. Tungsten oxide is yellow color solid and has a perovskite structure. A number of synthesis method has been used for preparing a thin film of $WO_3$ such as anodization[3], dip-coating[4], pulsed-laser deposition (PLD)[5], molecular beam epitaxy (MBE)[6], hydrothermal synthesis[7], thermal evaporation[8], chemical vapor deposition (CVD)[9], sputtering[10]. R Huang et al[11]. prepared $WO_3$ powder by the hydrothermal process and they studied the temperature effect on the morphological properties and photochromic characteristics of the sample. They

observed the best photochromic property was shown at 120º C. Ran Ji et al[12]. synthesized $WO_3$ by spray pyrolysis method and used it for solar cells as an anode buffer layer. C. Cantalini et al[13]. grow thin films of $WO_3$ by sol-gel method and detected a good response time of 1-2 minutes at 175 ppb towards oxygen gas. S. Yamamoto et al[14]. synthesized $WO_3$ epitaxial films by pulsed laser deposition method and they investigated the alteration in structural properties and gas chromic characteristics of the films. L. Santos et al.[15] fabricated $WO_3$ thin films by hydrothermal method and detected good sensitivity of biosensors based on tungsten oxides up to 2143 mA $M^{-1}$ $cm^{-2}$. The physical vapor deposition method like the Rf sputtering method is a significant technique that grows high-quality thin films on a large area. $WO_3$ thin film characteristics depend on the parameters such as the preparation technique and condition acquired during the thin film fabrications.

The variation in the microstructural characteristics of the sample originated from exposure such as fission fragments, alpha particles, X-rays, gamma rays and beta particles, it influences the optical and electrical properties of the target material. Gamma radiation consists of photons in which charge and mass are not present so it penetrates deeper as compared to any other radiation. It is also employed

in medical device sterilization to enhance the shelf life of foods and preservatives[16,17]. When gamma-ray interacts with the material it produces color centers in the sample and structural defects such as oxygen vacancy due to which variation in the density of defects were observed. The observed variation confirms the rate, radiation kind and interaction type with the target material. Gamma-ray interaction with material cause electronic excitation, ionization and displacement of an orbital electron. The variation in physical characteristics of the specimen by the effect of gamma radiation is used for device applications.[18] Various research groups study the variation in physical, optical, structural and morphological characteristics of various metal oxides under the effect of gamma radiation. Gouda et al.[19] study the effect of gamma radiation on PVA/PEDOT:PSS polymer composites and they observed the increment in conductivity of composites with the formation of a new phase inside the polymer. The gamma exposure to material alters electrical, thermal, and dielectric changes as well as the chemical structure of the polymer. Kovskaya et al.[20] study the change in the conductivity of $VO_2$ when exposed to gamma rays and they detected a reduction in the surface resistivity. Vattappalam et al.[21] chemically synthesize Al-ZnO nanocomposite and irradiate the sample with gamma rays, they found that the sensitivity of the sample increased after gamma irradiation as compared to the pristine sample. P. Sarkar et al.[22] prepared CuO thin films by the spray pyrolysis procedure and observed the alteration in optical, structural and morphological characteristics of the sample after gamma irradiation. Maqsood R. Waikar et al.[23] synthesize ZnO thin films by chemical bath deposition (CBD) and treated with gamma radiation and they investigated good sensing performance with a response factor of 7.29 as compared to a virgin sample. N. Lavanya et al.[24] prepared $WO_3$ sample by microwave technique and exposed it to gamma source with doses of 0 kGy, 50 kGy and 100 kGy and found the variation in the characteristics like structural, gas sensing electrical properties after the gamma irradiation.

From the literature, we concluded that no work has been done to study the effect of high-gamma doses on $WO_3$ thin films. The motive of our work is to study the consequences of high-dose gamma on structural, morphological and optical characteristics of $WO_3$ thin films and gamma radiation at such a high dose has not been performed before. Our work will be useful for

technological applications in immoderate gamma environment conditions.

## 2 Materials and Methods

$WO_3$ thin films were deposited on silicon and glass substrate by RF sputtering technique at MNIT Jaipur. The deposition parameter during the sputtering is shown in Table 1. Then synthesized $WO_3$ thin films were treated by gamma radiation with different doses of 600 kGy, 1000 kGy and 1250 kGy Inter-University Accelerator Centre, New Delhi (IUAC).

After the gamma treatment of $WO_3$ thin film with different doses, we study the alteration in morphological, optical and structural properties by Photoluminescence spectroscopy (PL ), Atomic Force Microscopy, Raman Spectroscopy, UV-Visible Spectroscopy and X-Ray Diffraction (XRD).

## 3 Results and Discussion

### 3.1 X-Ray Diffraction

XRD spectra of pristine and gamma-exposed $WO_3$ thin films at 600 kGy, 1000 kGy and 1250 kGy are shown in Fig. 1. From Fig, we can observe different peaks at angles 24.4º, 34.3º, 41.5º, 50.1º and 56.0º with the corresponding crystal planes (200), (220), (222), (232) and (420) show the monoclinic structure

Table 1 — Deposition Parameters of $WO_3$ thin films during sputtering

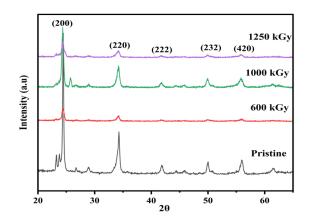| | |
|---|---|
| Power | 100 W |
| Ar gas flow rate | 15 Sccm |
| Rotation rate | 10-12 rpm |
| Working pressure | $3 \times 10^{-2}$ mbar |
| Distance between target and substrate | 8 cm |
| Temperature | Room temperature |
| Base Pressure | $1.64 \times 10^{-5}$ mbar |



Fig.1 — XRD spectra of Un-irradiated and gamma treated $WO_3$ thin at various doses.

of un-irradiated and gamma-irradiated $WO_3$ thin films. The XRD peaks are well matched with the precedent-reported result with JCPDS No. 43–1035.[25] After the gamma treatment of thin films, the peak intensity decreases which may be due to structural disorders produced by the effect of irradiation such as oxygen vacancy and color center.[26] The crystallite size of pristine and gamma treated thin films of $WO_3$ were measured by the following equation

$$D = k\lambda/\beta\cos\theta \qquad \qquad \dots(1)$$

The value of D varies from 32.02 nm to 13.76 nm when thin films were irradiated with gamma radiation as displayed in Table 2. The decrement in the size of crystals is attributed to the displacement of an atom from its position by penetration of gamma photon in material and as a result, the molecule breaks into smaller ones which reduces crystallite size.[27] The dislocation density and strain were measured by the following relations[28]

$$\delta = 1/D^2 \ (2) \qquad \qquad \dots (2)$$
$$\varepsilon = \beta /4 \ tan\theta \qquad \qquad \dots (3)$$

The alteration in dislocation density and the strain was observed after gamma treatment at different doses as shown in table 2. The defects such as oxygen vacancy and dislocations cause the variation in strain from 1.92 to 5.77 which takes place due to a reduction in the size of crystallites.[29]

### 3.2 UV-Visible Spectroscopy

The optical study of un-irradiated and gamma-treated $WO_3$ thin films was done by UV-Visible spectroscopy. UV-visible spectra are used for measuring various variables like absorbance, optical band gap, Urbach energy, skin depth and extinction coefficient. The absorbance and band gap of virgin and gamma-treated $WO_3$ thin films are displayed in Fig. 2. The absorbance of $WO_3$ thin film increases at 1250 kGy dose. The enhancement in the absorbance after gamma irradiation was observed because of oxygen vacancy produced in the thin films and electron migrates to the conduction band causing powerful absorption of photons.[30]

The band gap of virgin and gamma-treated $WO_3$ thin films at distinct doses is observed by Tauc relation[31]

$$(\alpha\upsilon)^k = A(h\upsilon - E_g) \qquad \qquad \dots (4)$$

Where $\alpha$ is the coefficient of absorption, $h\upsilon$ is the energy of the photon and $E_g$ is the optical energy band

Table 2 — The estimated value of crystallite size, dislocation density, and lattice strain of unirradiated and gamma treated $WO_3$ thin films for the plane (220) at various doses.

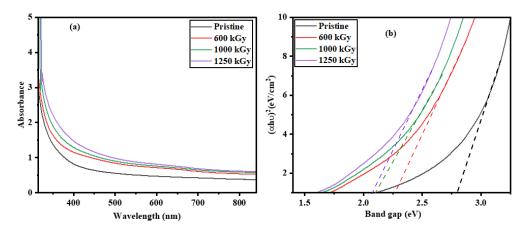| Dose (kGy) | FWHM (radians) | Crystallite Size (nm) | Dislocation Density ($\delta$) ($\times 10^{16}$ m$^{-2}$) | Strain ($\times 10^{-3}$) |
|---|---|---|---|---|
| Pristine | 0.0052 | 32.02 | 9.7534 | 1.92 |
| 600 kGy | 0.0069 | 24.03 | 0.0017 | 2.56 |
| 1000kGy | 0.0073 | 21.02 | 0.0020 | 3.25 |
| 1250 kGy | 0.0157 | 13.76 | 0.0052 | 5.77 |



Fig. 2 — (a) Absorbance versus wavelength (b) optical band gap of Un-irradiated and gamma treated $WO_3$ thin film at various doses.

gap of the material. The k value determines the transition nature of the material, for k=1/2 it posses an indirect band gap and for k=2 represents direct band gap. The plot of photon energy versus (αhυ) is displayed in Fig 2(b). Optical energy band gap of un-irradiated and gamma-treated $WO_3$ thin film is given in table 3. Un-irradiated $WO_3$ thin film exhibits a band gap of 2.80 eV and after gamma treatment at a higher dose of 1250 kGy it becomes 2.08 eV. The value of the band gap decrease after gamma irradiation is attributed to variations in the size of the crystal and defects in the crystal. The defects in the material produce localized states which reduce the optical band gap after gamma irradiation of the thin films.[32]

### 3.2.1 Urbach Energy

Urbach energy is a significant parameter that illustrates all defects present in the sample. Urbach energy value is based on various parameters such as point defects, structure disorder and strain in the sample. Urbach energy is calculated by the following relation[33]

$$\alpha = \alpha_0 \exp(h\nu/E_U) \qquad \qquad \dots(5)$$
$$\ln\alpha = \ln\alpha_0 + (h\nu/E_U) \qquad \qquad \dots(6)$$

where $E_U$ represents Urbach energy, $h\nu$ is photon energy and $\alpha$ is constant. Fig. 3(a). displays the plot of photon energy and lnα. Un-irradiated $WO_3$ thin film shows Urbach energy of 1.128 eV and after exposure to gamma irradiation, it becomes 1.250 eV as displayed in Table 3. The variation in Urbach energy after gamma irradiation may be due to enhancement in the defects generation which also generates localized states in the band gap.[34]

### 3.2.2 Skin depth and extinction coefficient

Skin depth and extinction coefficient plot of un-irradiated and gamma-treated thin films of $WO_3$ at various doses is given in Fig. 3(b) and 3(c). Skin depth is associated with the absorption phenomena and is also named penetration depth. The value of energy at which photon energy completely vanishes is known as cut-off energy. Un-irradiated $WO_3$ thin film shows cut-off energy of 3.95 eV. The extinction coefficient of un-irradiated and gamma-treated $WO_3$ thin films are measured by the relation k=α λ /4π.[35] The variation in extinction coefficient was observed after gamma treatment of $WO_3$ thin films due to microstructural and morphological changes occurring in thin films.

Table 3 — The Direct band gap and Urbach energy of Un-irradiated and gamma treated $WO_3$ thin film.

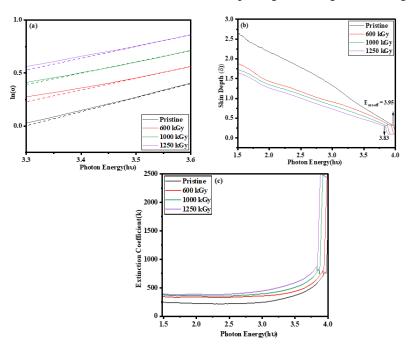| Doses | Direct Band Gap (eV) | Urbach Energy (meV) |
|---|---|---|
| Pristine | 2.80 | 1.128 |
| 600 kGy | 2.26 | 1.269 |
| 1000 kGy | 2.11 | 1.257 |
| 1250 kGy | 2.08 | 1.250 |



Fig. 3 — Plot of (a) Urbach Energy, (b) Skin Depth, and (c) Extinction Coefficient of Un-irradiated and gamma treated $WO_3$ thin film at different doses.

### 3.3 Photoluminescence Spectroscopy

PL spectra of the virgin and $WO_3$ gamma exposed films were studied at room temperature with an excitation wavelength of 380 nm with different doses. The emission spectra of $WO_3$ thin films were taken in the wavelength region of 400-550 nm as displayed in Fig. 4. The electrons move to the conduction band because of the UV-illumination process and some of the electrons remain in the low energy levels, these remaining electrons can not return from the surface states to the valence band. The surface state is produced by defects in the sample which results in radiative transition by surface states. The excitation wavelength provides suitable details of defects present in the material. The emission spectra of un-irradiated $WO_3$ thin films and gamma-exposed thin films at 600kGy, 1000 kGy and 1250 kGy were obtained at wavelengths of 410 nm and 480 nm with the energy of 3.02 eV and 2.58 eV. The emission peak at 410 and 480 nm is consistent with the blue emission band. The observed blue emission band is because of the band-to-band transition of the tungsten oxide structure. The emission band near UV visible region at 410 nm and 480 nm is observed because of oxygen vacancy in the material.[36] The PL intensity at 600 kGy, 1000 kGy and 1250 kGy attenuated after gamma irradiation is attributed to the reduction in crystallite size. The PL intensity reduces because of the production of defects which enhances the non-radiative recombination rate with gamma doses.[37]

### 3.4 Raman Spectroscopy

Raman spectroscopy of the pristine $WO_3$ and gamma-irradiated thin film are displayed in Fig. 5. The Raman spectra show two Raman bands in the region of 200 to 500 $cm^{-1}$ and another one from 500 to 1000 $cm^{-1}$. The Raman band at 274 nm was observed only for 200 nm thickness of un-irradiated and gamma-exposed $WO_3$ thin films. This band displays the stretching mode of oxygen such as single bond $O-W^{6+}-O$ and distortion of O-W-O bond. The Raman peak at 717.2 and 807.6 $cm^{-1}$ correspond to stretching vibration and the Raman band at 329.7 shows the presence of bending vibration in the pristine and gamma-treated $WO_3$ thin films. The Raman peak observed at 521 $cm^{-1}$ shows the presence of silicon. We found that Raman spectra are matched with the reported results and $WO_3$ shows a monoclinic structure before and after gamma treatment at different doses.[38] The Raman intensity increases may be due to enhancement in grain size as consistent with AFM results.[39]
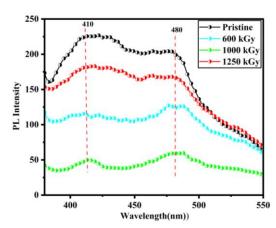


Fig. 4 — PL spectra of Unirradiated and gamma treated $WO_3$ thin films at various doses.
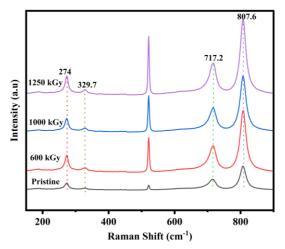


Fig. 5 — Raman spectra of Unirradiated and gamma treated $WO_3$ thin films at distinct doses.

### 3.5 Atomic Force Microscopy

The morphological study of un-irradiated and gamma-exposed $WO_3$ thin film at different doses was done by AFM spectroscopy. The 3-D and 2-D images of un-irradiated and gamma-exposed $WO_3$ thin film are shown in Fig. 6. Pristine $WO_3$ shows a roughness of 143 nm and after gamma treatment at 1250 kGy, it becomes 41.3 nm. At a higher dose of 1250 kGy, the roughness decreases because more defects are produced because of the high dose of gamma irradiation which further increases surface diffusion.[40]

The size of grains for pristine and gamma-treated $WO_3$ thin films was measured by Gwaddiyon software. The size of grains varies from 61 nm to 91.2 nm from virgin to gamma-treated $WO_3$ thin films. The increment in grain size was observed because high-dose irradiation melts the small-size particles and produces a quenching effect. The growth of grain takes place due to decreases in the crystallinity of the
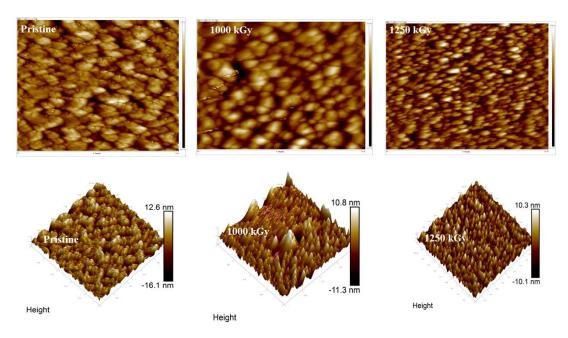
Fig. 6 — 2D and 3D image of un-irradiated and gamma-exposed $WO_3$ thin film at varying doses.

sample with the gamma treatment and causes an increase in the density of defects.[41]

## 4 Conclusion

RF sputtered deposited $WO_3$ thin films was irradiated by Co-60 source with different doses at 600 kGy, 1000 kGy and 1250 kGy. The roughness of the $WO_3$ thin films varies from 143 nm to 41.3 nm. The size of the grain was enhanced from 61 nm to 91.2 nm after treating the $WO_3$ thin films with gamma radiations. The variation in grain size is due to defects created during gamma irradiation. The X-ray diffraction shows the decrement in the size of the crystal from 32.02 nm to 13.76 nm after the gamma radiation treatment on $WO_3$ thin films. In PL spectroscopy emission peaks were found at 410 and 480 nm before and after gamma exposure, the PL intensity was reduced due to the generation of defects which enhance the recombination rate. The decrement in PL intensity at high doses may be due to the production of new defects and primary defects annihilation at higher fluence. From the optical study, several properties of $WO_3$ thin film were studied such as absorbance, Urbach energy, extinction coefficient and skin depth. The alteration in absorbance of $WO_3$ thin after gamma irradiation was observed and the band gap alteration after gamma treatment of $WO_3$ thin films was observed in the region from 2.80 eV to 2.08 eV. The maximum Urbach energy is found to be 1.269 meV for 600 kGy and a minimum value of 1.128 meV for pristine $WO_3$ thin films. Raman spectra of the virgin and gamma-exposed samples show the monoclinic structure with a prominent peak at 807.06 cm$^{-1}$.

## References

1    Manikanthababu, N, V Saikiran, T Basu, K Prajna, S Vajandar, A P Pathak, B K Panigrahi, T Osipowicz, & SVS Nageswara Rao, *Thin Solid Films*, 682 (2019) 156.
2    Wang, Zishuai, Ming Hu, Yifei Wang, Xiangcheng Liu &Yuxiang Qin, *J Alloys Compd,* 665 (2016) 173.
3    Levinas, R, N Tsyntsaru, M Lelis, & H Cesiulis, *Electrochim Acta,* 225 (2017) 29.
4    Shieh, Jiann, H M Feng, Min-Hsiung Hon, & H Y Juang, *Sens Actuators B Chem*, (2002) 75
5    Boyadjiev, Stefan I, Velichka Georgieva, Nicolaie Stefan, George E Stan, Natalia Mihailescu, Anita Visan, Ion N Mihailescu, Cristina Besleaga, &Imre M Szilágyi, *Appl Surf Sci*, 417 (2017) 218.
6    Li, Guoqiang, Tamas Varga, Pengfei Yan, Zhiguo Wang, Chongmin Wang, Scott A Chamber & Yingge Du, *Phys Chem Chem Phys* 17 (23) (2015) 15119.
7    Zhang, Jun, Jiang-ping Tu, Xin-hui Xia, Xiu-li Wang & Chang-dong Gu, *J Mater Chem*, 21(14) (2011) 5492.

8   Li, Shenghao, Zhirong Yao, Jixiang Zhou, Rui Zhang & Hui Shen, *Mater Lett*, 195 (2017): 213.

9   Godbole, Rhushikesh, Sadia Ameen, Umesh T Nakate, M Shaheer Akhtar & Hyung-Shik Shin, *Mater Lett*, 254 (2019) 398.

10  Marszalek, Konstanty, *Thin Solid Films*, 175 (1989): 227.

11  Huang, Rong, Yi Shen, Li Zhao & Minyan Yan, *Adv Powder Technol*, 23(2) (2012) 211.

12  Ji, Ran, Ding Zheng, Chang Zhou, Jiang Cheng, Junsheng Yu, & Lu Li, *Materials* 10(7) (2017)820.

13  Cantalini, C, W Wlodarski, Y Li, M Passacantando, S Santucci, E Comini, G Kaur, Ravneet, Surinder Singh, & O P Pandey, *J Mol Struct*, 1048 (2013) 78.

14  Gouda, M E, &Elrasasi, T Y, *J Appl Phys*, (2015) 7(6), 22.

15  Kaurkovskaya, V N, A P Shakhov, V V Lobanov, & I R Entinzon, High Energy Chem, 44 (2 ) (2010) 101.

16  Vattappalam, Sunil C, Deepu Thomas, Simon Augustine, & Sunny Mathew, *Cogent Physics* 2,(1) (2015) 1019664

17  Sarker, Pooja, Sapan Kumar Sen, M N H Mia, M F Pervez, A A Mortuza, Sazzad Hossain, & M F Mortuza, *Ceram Int* , 47(3) (2021) 3626.

18  Waikar, Maqsood R, Pooja M Raste, Rakesh K Sonker, Vinay Gupta, Monika Tomar, Mahendra D Shirsat, & Rajendra G Sonkawade, *J Alloys Compd*, 830 (2020) 154641.

19  Lavanya, N, A C Anithaa, C Sekar, K Asokan, A Bonavita, N Donato, S G Leonardi, & G Neri, *J Alloys Compd*, 693 (2017) 366.

20  Miyakawa, M, Ueda, K, & Hosono, *J Appl Phys*, (2002) 92(4), 2017.

21  El-Nahass, M M, A A M Farag,& A A Atta, *Synth Met*159 (7-8) (2009) 589.

22  Deepika, Gupta D, Vishnu Chauhan, Aman Mahajan, Rashi Gupta, S Asad Ali, & Rajesh Kumar, *Radiat Phys Chem* ,202 (2023) 110554.

23  Sarmah, K, Sarma, R, & Das, H L, Chalcogenide Lett, (2008) 5(8), 153.

24  Abhirami KM, Sathyamoorthy R, & Asokan K, *Radiat Phys Chem* (2013) 91, 35.

25  Jaiswal, MK, Kumar, R, Kanjilal, D, Dong, CL, Chen, CL, Asokan, K & Ojha, S, Appl Surf Sci, 2015(332) 726.

26  Zhang W, Fan Y, Yuan T, Lu B, Liu Y, Li Z, Li G, Cheng Z, Xu & J, ACS *Appl Mater Interfaces* (2020) 12 (2020) 3755.

27  El-Korashy, A, *Radiat Eff Defects Solids* 153( 2) (2001) 139.

28  Ilican, S, Caglar, Y, &Caglar, M (2008) 10(10), 2578.

29  Ahmad, Shabir, K Asokan, & M Zulfequar, *Philos.Mag,* 95(12) (2015) 1309.

30  Yu, W W, Qu, L, Guo, W, & Peng X, *Chem Mater*, (2003) 15(14), 2854.

31  Wang, F, Di Valentin, C, &Pacchioni, G, *Phys. Rev. Appl B*, (2011) 84(7), 073103.

32  Nagabhushana, K R, Lakshminarasappa, B N, Chandrappa, G T, Haranath, D, & Singh, F *Radiat. Eff. Defects Solids*, (2007) 162(5), 325.

33  Lin, YS, Chen, HT Wu, SS, J Solid State Electrochem, 2010 14(10), pp1885-1895

34  Karuppasamy, A, *Appl Surf Sci*, 282 (2013) 77.

35  P K, Singh, F (2008), 266(8), 1475.

36  Jaiswal, MK, Kumar, A, Kanjilal, D and Mohanty, T, *Appl Surf Sci*, 282 (2012), 586.